Simulations of Turbulent Momentum and Scalar Transport in Confined Swirling Coaxial Jets

Tsan-Hsing Shih
Ohio Aerospace Institute, Cleveland, OH 44142

Nan-Suey Liu and Jeffrey P. Moder
NASA Glenn Research Center, Cleveland, OH 44135

Objective

- Validate the newly proposed nonlinear turbulence models for momentum and scalar transport
- Evaluate the newly proposed scalar joint probability density functions (APDF and DWFDF) along with its Eulerian method in the National Combustion Code (NCC).
- Simulations conducted include
  - Steady Reynolds averaged Navier-Stokes RANS,
  - Unsteady RANS (URANS)
  - Time-filtered Navier-Stokes (TFNS) --- very large eddy simulation
  - Hybrid RANS/APDF
  - Hybrid URAND/APDF
  - Hybrid TFNS/DWFDF --- very large eddy simulation

In the hybrid scheme, the transport equations of energy and species are replaced by the APDF or DWFDF equation

Some positive effects of nonlinear models and hybrid approaches observed.

Confined Swirling Coaxial Jets

Geometry configuration

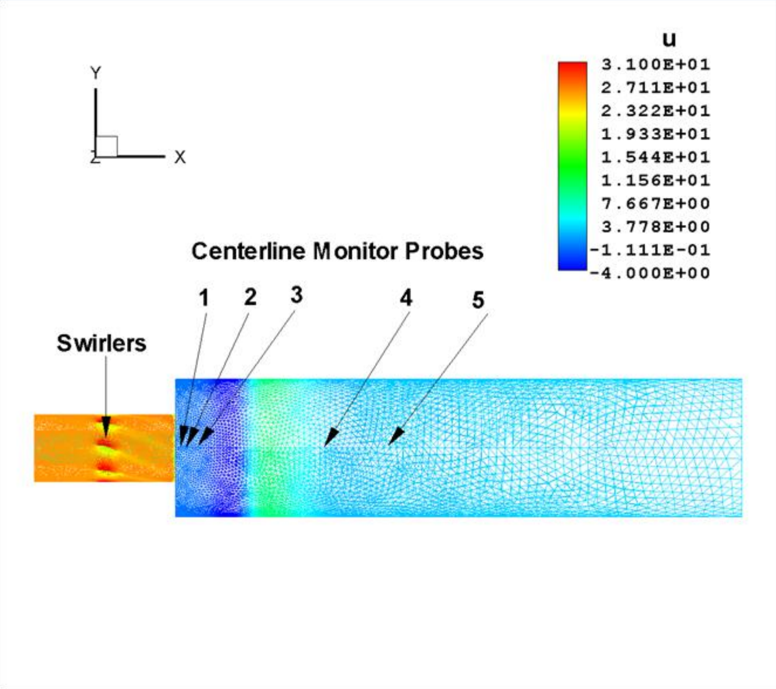

Swirler

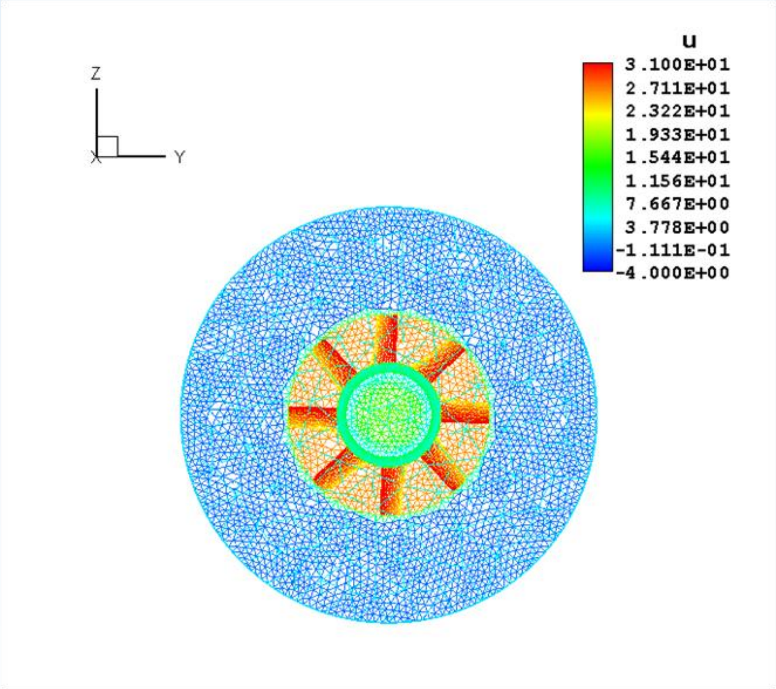

Computational domain and grid

849,189 tetrahedral elements

Simulation of water jet using NCC

- Experiments are water jets.
- NCC code is for ideal gas flow.
- “Reynolds number similarity law” under low speed conditions was used for rescaling between the water and gas flows.

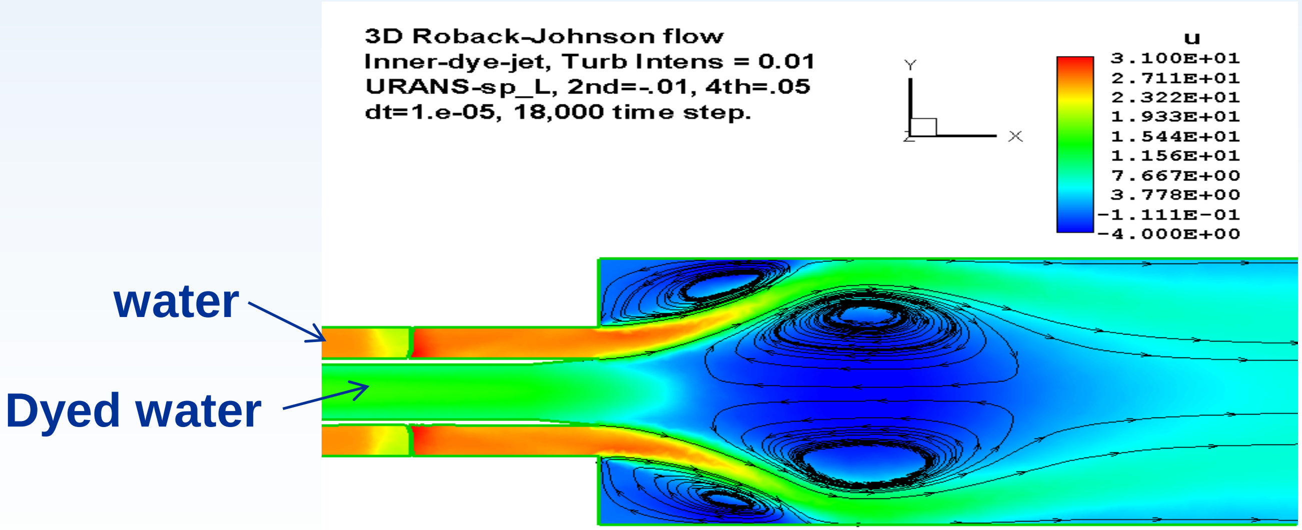

Outline

- Basic equations for RANS, URANS and TFNS.
- Scalar APDF and DWFDF equation for hybrid approach.
- Comparison of numerical simulations with experimental data.
- Conclusions.

Equations for RANS, URANS and TFNS

$$\frac{\partial\bar{\rho}}{\partial t}+\frac{\partial\,\bar{\rho}U_j}{\partial x_j}=0$$

$$\frac{\partial\bar{\rho}U_i}{\partial t}+\frac{\partial\,\overline{\rho U_i U_j}}{\partial x_j}=-\frac{\partial\bar{P}}{\partial x_i}+\frac{\partial}{\partial x_j}\left[\nu\left(\frac{\partial\bar{\rho}U_i}{\partial x_j}+\frac{\partial\bar{\rho}U_j}{\partial x_i}-\frac{2}{3}\delta_{ij}\frac{\partial\bar{\rho}U_k}{\partial x_k}\right)\right]$$

$$\frac{\partial\bar{\rho}\,\tilde{e}}{\partial t}+\frac{\partial\,\overline{\rho U_i e}}{\partial x_i}=-\frac{\partial\bar{q}_i}{\partial x_i}+\overline{PS_{kk}}+\bar{\rho}\,\tilde{\varepsilon}+\bar{Q}$$

$$\frac{\partial\bar{\rho}\,\Phi_m}{\partial t}+\frac{\partial\overline{\rho U_i\Phi_m}}{\partial x_i}=\frac{\partial}{\partial x_i}\left(\Gamma^{(m)}\frac{\partial\bar{\rho}\,\Phi_m}{\partial x_i}\right)+\overline{\rho S_m}\qquad m=1,2,\cdots,M$$

$$\bar{P}=\overline{\rho R\sum_{m=1}^{M}\frac{\Phi_m T}{w_m}}=\overline{\left(\frac{\rho RT}{\bar{M}}\right)}\approx\frac{\bar{\rho}RT}{M}\approx\frac{\bar{\rho}R\,\Phi_{M+1}}{c_\upsilon M},\quad \frac{1}{\bar{M}}=\sum_{m=1}^{M}\frac{\Phi_m}{w_m},\quad \frac{1}{M}=\sum_{m=1}^{M}\frac{\Phi_m}{w_m}$$

$$\bar{q}_i\approx-\frac{\kappa}{\bar{\rho}}\frac{\partial\bar{\rho}T}{\partial x_i}$$

$$\bar{\phi}(\mathbf{x},t)=\int_{-\infty}^{+\infty}\phi(\mathbf{x},t)G(t-t')\,dt',\qquad \phi(\mathbf{x},t)=\frac{\overline{\rho\phi}}{\bar{\rho}}$$

Nonlinear models

- $\bar{\rho} U_i U_j$, $\bar{\rho} U_i e$, $\bar{\rho} U_i \Phi_m$ **can be expressed through the following turbulent transports (stresses and scalar fluxes)** τ_{ij}, Θ_i :

$$\tau_{ij} \equiv \bar{\rho}(U_i U_j - \tilde{U}_i \tilde{U}_j), \quad \Theta_i \equiv \bar{\rho}(U_i \theta - \tilde{U}_i \tilde{\theta}).$$

- **Nonlinear models are (NASA/TM-1997-113112, 2010-216323):**

$$\tau_{ij} = \frac{1}{3}\delta_{ij}\tau_{kk} - 2C_\mu \cdot f \cdot \bar{\rho}\frac{k^2}{\varepsilon}\left(\tilde{S}_{ij} - \delta_{ij}\tilde{S}_{kk}/3\right) - A_3 \cdot f \cdot \bar{\rho}\frac{k^3}{\varepsilon^2}\left(\tilde{S}_{ik}\tilde{\Omega}_{kj} - \tilde{\Omega}_{ik}\tilde{S}_{kj}\right)$$

$$+2A_5 \cdot f \cdot \bar{\rho}\frac{k^4}{\varepsilon^3}\left[\tilde{\Omega}_{ik}\tilde{S}_{kj}^2 - \tilde{S}_{ik}^2\tilde{\Omega}_{kj} + \tilde{\Omega}_{ik}\tilde{S}_{km}\tilde{\Omega}_{mj} - \tilde{\Omega}_{kl}\tilde{S}_{lm}\tilde{\Omega}_{mk}\delta_{ij}/3 + II_s(\tilde{S}_{ij} - \delta_{ij}\tilde{S}_{kk}/3)\right],$$

$$\Theta_i = -\vartheta_T \frac{\partial \bar{\rho}\,\tilde{\theta}}{\partial x_i} - \vartheta_T \frac{k}{\varepsilon}\left(c_1\tilde{S}_{ij} + c_2\tilde{\Omega}_{ij}\right)\frac{\partial \bar{\rho}\,\tilde{\theta}}{\partial x_j}$$

where $f = 0 \le f(RCP) \le 1$, $0 \le RCP \le 1$ --- Resolution control parameter.

Equation for Scalar APDF & DWFDF, $F_\Phi(\psi\,;\,\boldsymbol{x},t)$

A density weighted ensample averaged or time filtered fine grained scalar PDF, $F_\Phi(\psi\,;\,\boldsymbol{x},t)$, is defined as:

$$F_\Phi(\psi\,;\,\boldsymbol{x},t) \equiv \int_{-\infty}^{+\infty} \rho\left(\boldsymbol{x},t'\right) f_\Phi^{'}(\psi\,;\,\boldsymbol{x},t')\,G(t-t')\,dt'$$

where, $f_\Phi^{'}(\psi\,;\,\boldsymbol{x},t') \equiv \delta\left(\boldsymbol{\Phi}\left(\boldsymbol{x},t'\right)-\psi\right)$ --- fine grained scalar PDF

With above definition, the density weighted mean or filtered variable $\boldsymbol{\Phi}$ can be fully expressed using $F_\Phi(\psi\,;\,\boldsymbol{x},t)$ as:

$$\int_{-\infty}^{+\infty} \psi\, F_\Phi(\psi\,;\,\boldsymbol{x},t)\,d\psi = \overline{\rho\,\boldsymbol{\Phi}} = \bar{\rho}\left(\boldsymbol{x},t\right)\boldsymbol{\Phi}(\boldsymbol{x},t)$$

Insert this relationship into scaler transport equation, we will obtain a transport equation for scalar $F_\Phi(\psi\,;\,\boldsymbol{x},t)$:

- The resulting transport equation for $F_\Phi(\boldsymbol{\psi};\boldsymbol{x},t)$ is

$$\frac{\partial F_\Phi}{\partial t}+\frac{\partial\left(U_i F_\Phi\right)}{\partial x_i}=\left\{\frac{\partial}{\partial x_i}\left(\left(\Gamma^{(m)}+\Gamma_T^{(m)}\right)\frac{\partial F_\Phi}{\partial x_i}\right)\right\}-\frac{\partial}{\partial \psi_k}\left(F_\Phi\cdot S_k\left(\boldsymbol{\psi}\right)\right)$$

$$-\frac{\partial}{\partial \psi_k}\left\{\psi_k\frac{\partial}{\partial x_i}\left(\Gamma_T^{(m)}\frac{k}{\varepsilon}\left(c_1 S_{ij}+c_2\Omega_{ij}\right)\frac{\partial F_\Phi}{\partial x_j}\right)\right\},\quad k=1,2,\cdots,M+1$$

Note that the chemical reaction term $S_k\left(\boldsymbol{\psi}\right)$ is in a closed form!

- The diffusion term in the sample space is further simplified to fit the available PDF solution procedure built in NCC code as

$$-\frac{\partial}{\partial \psi_k}\left\{\psi_k\frac{\partial}{\partial x_i}\left(\Gamma_T^{(m)}\frac{k}{\varepsilon}\left(c_1\tilde{S}_{ij}+c_2\Omega_{ij}\right)\frac{\partial F_\Phi}{\partial x_j}\right)\right\}\approx\frac{\partial}{\partial \psi_k}\left(\psi_k\frac{1}{\tau}F_\Phi\right)$$

$$\textit{where},\quad \frac{1}{\tau}\equiv\sqrt{\tilde{S}_{ij}\tilde{S}_{ij}+\Omega_{ij}\Omega_{ij}}$$

Results of simulations and comparisons

Global flow features of TFNS (VLES) simulation

Scalar flux model: linear

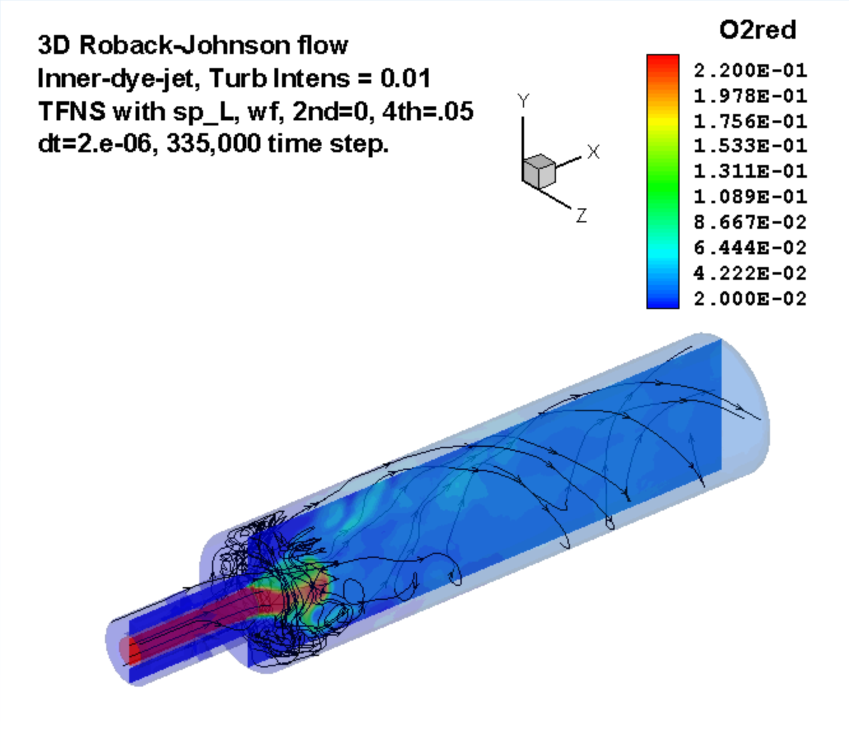

Scalar flux model: non-linear

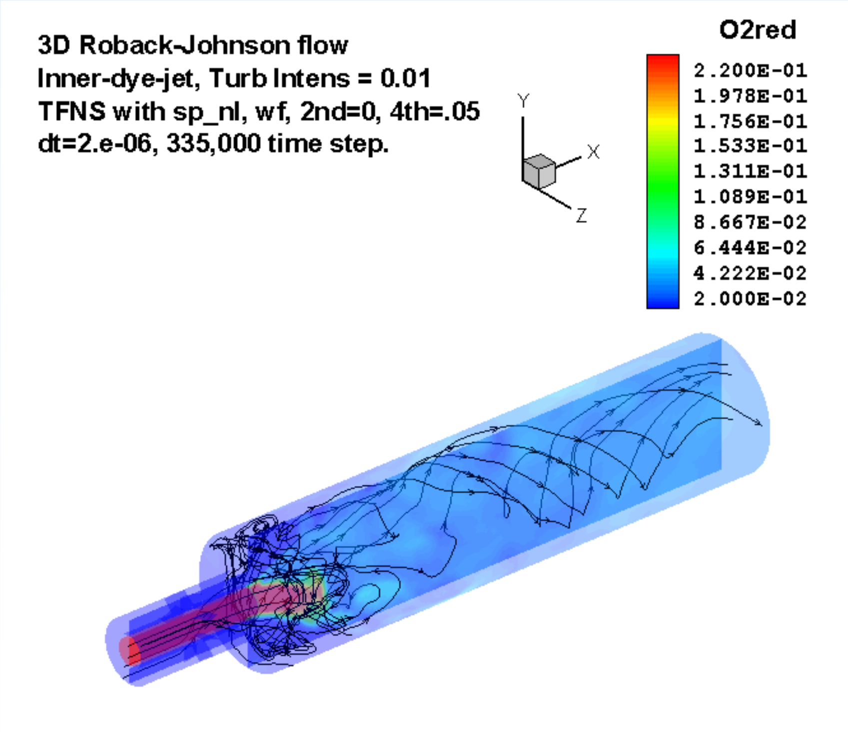

Time history of velocity components u, v, w at probe 4

Scalar flux model: linear

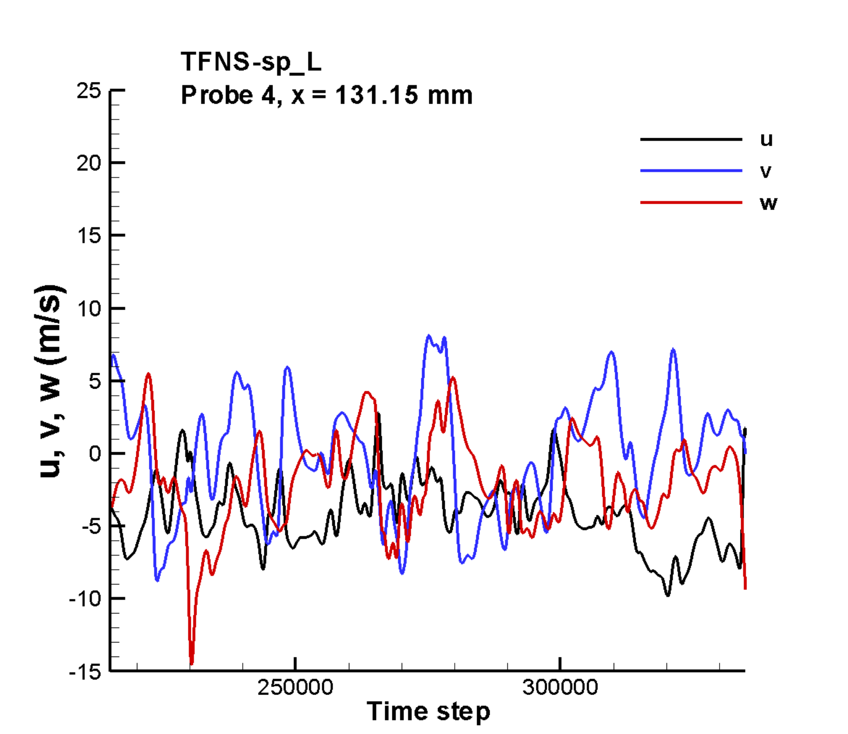

Scalar flux model: non-linear

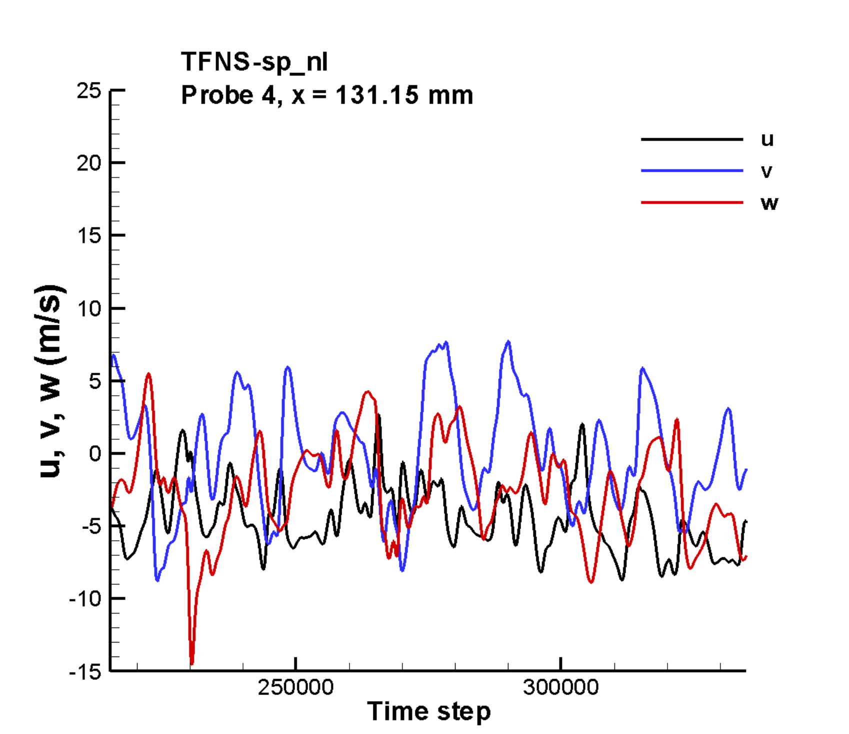

Vortex brake-down Bubble

Scalar flux model: linear

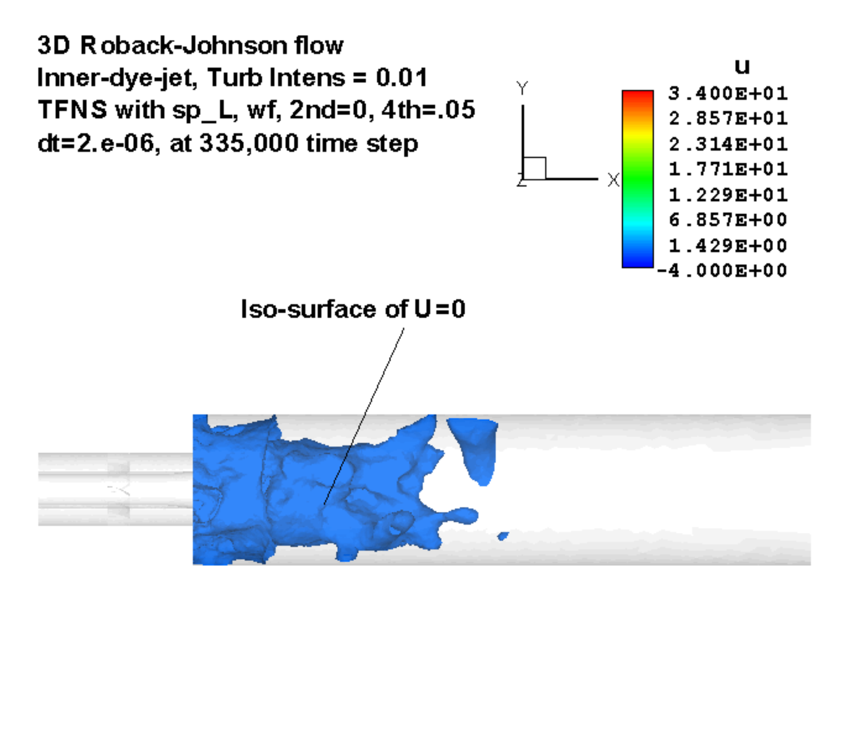

Scalar flux model: non-linear

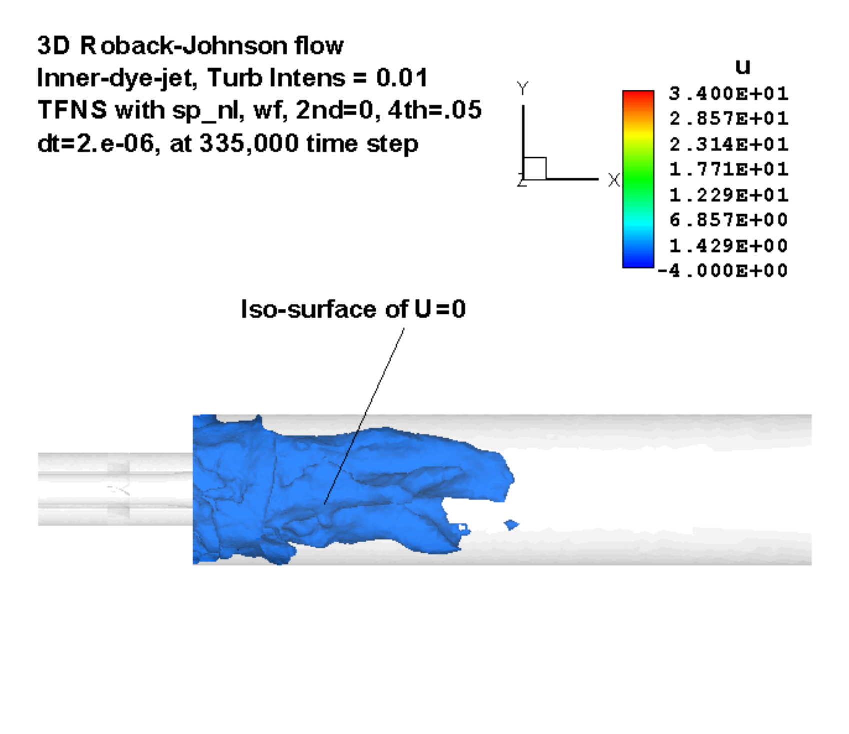

Contour of instant axial velocity, u

Scalar flux model: linear

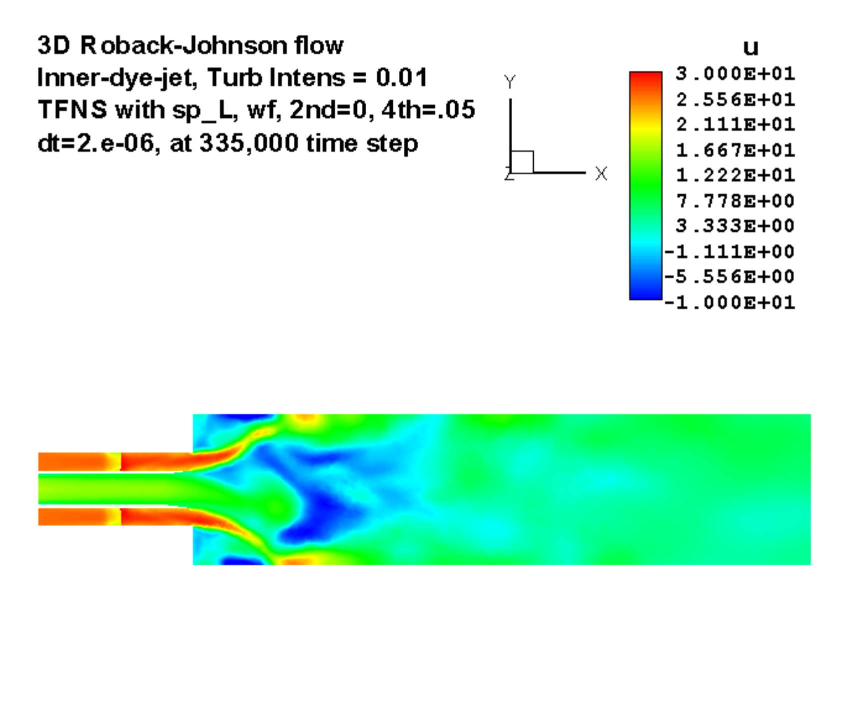

Scalar flux model: non-linear

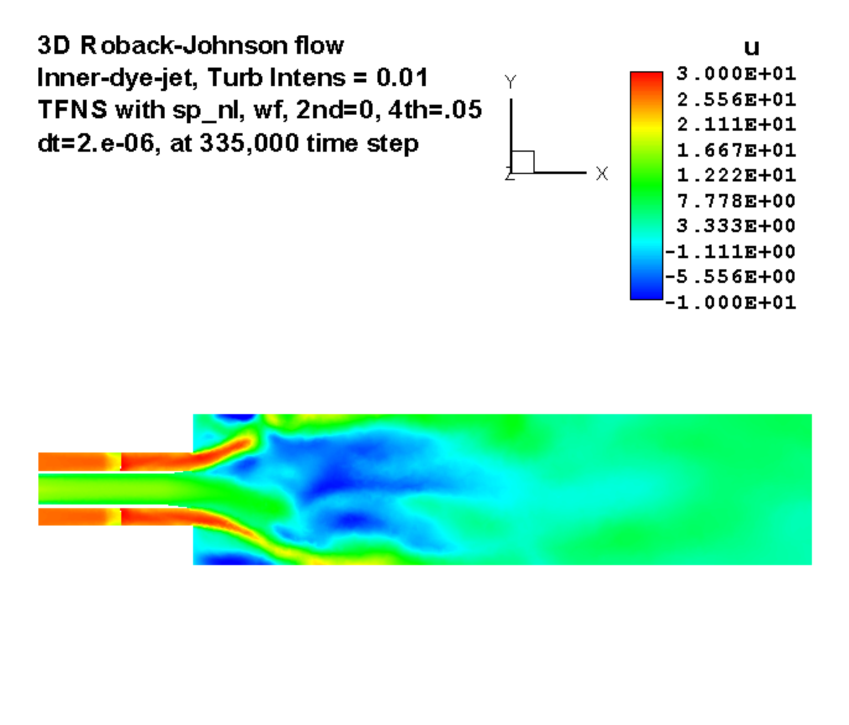

Contour of colored O2 concentration

Scalar flux model: linear

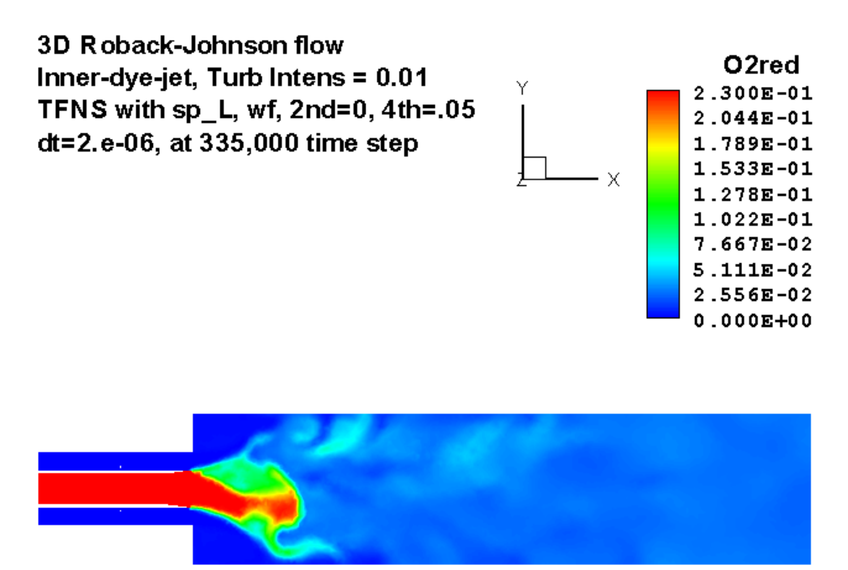

Scalar flux model: non-linear

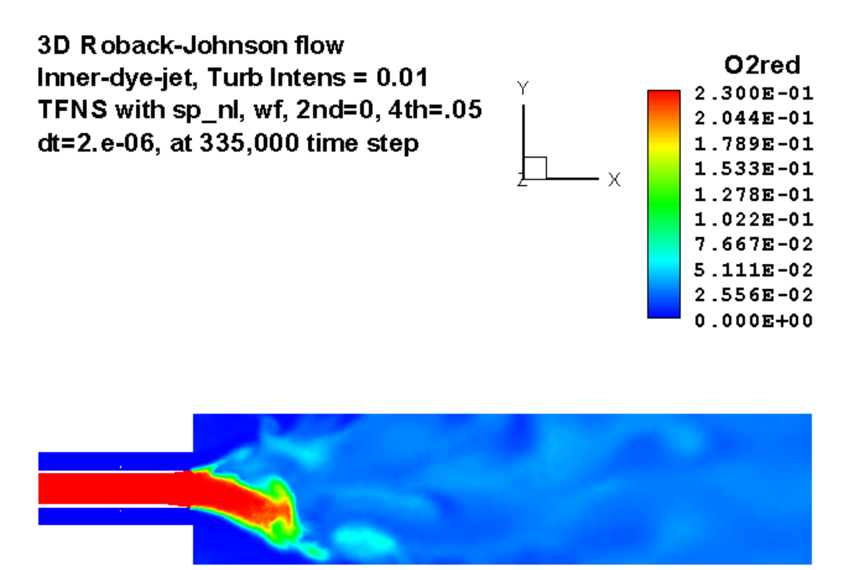

Contour of effective viscosity, mu

Scalar flux model: linear

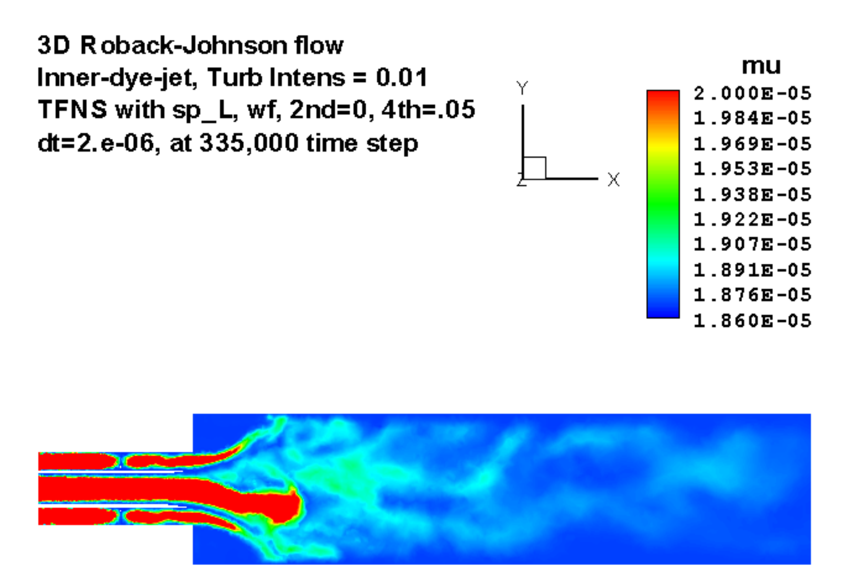

Scalar flux model: non-linear

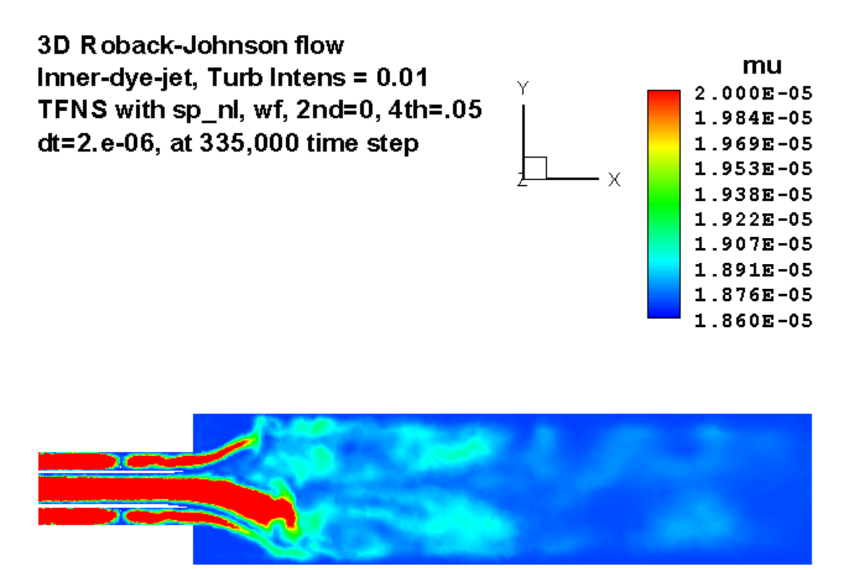

Contour of vorticity magnitude

Scalar flux model: linear

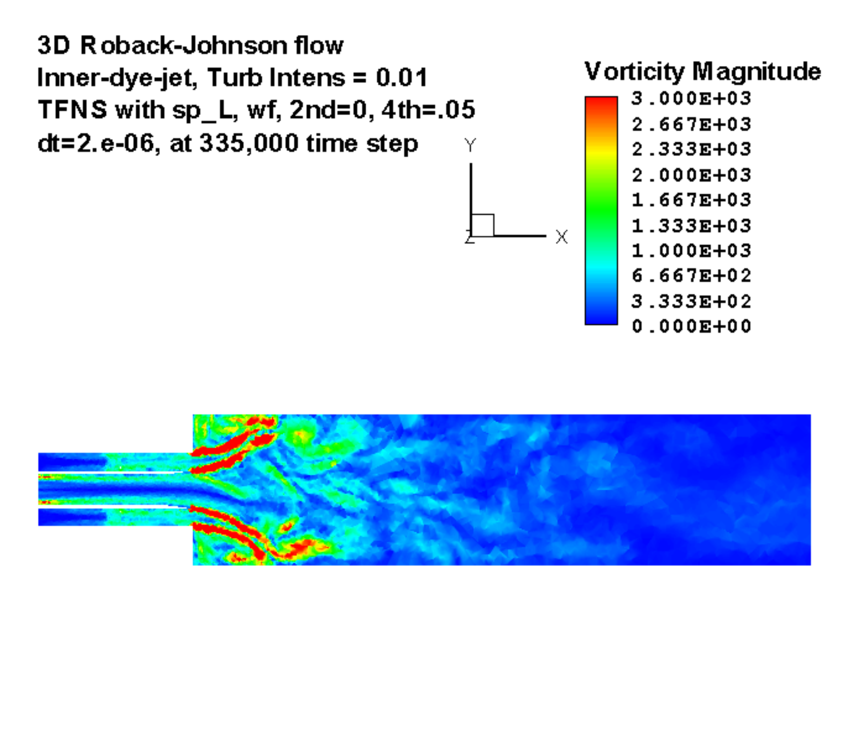

Scalar flux model: non-linear

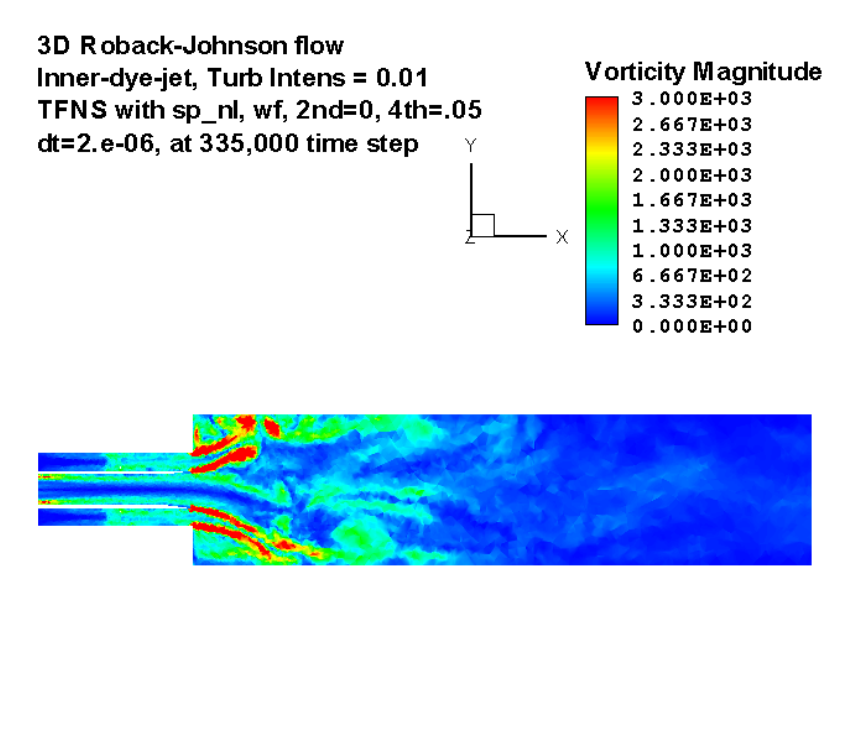

URANS simulation

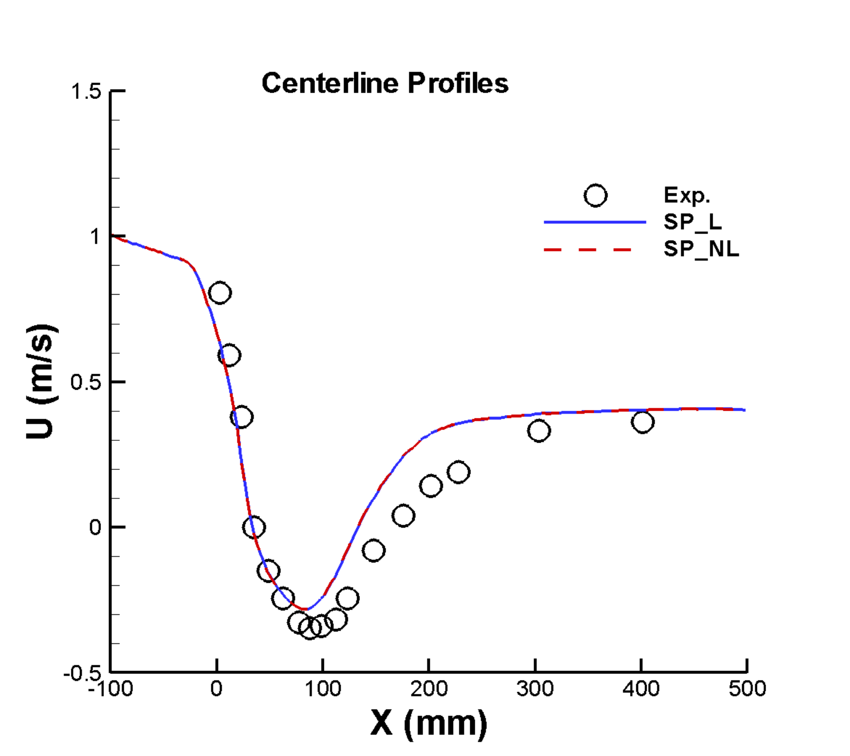

URANS: Axial velocity along centerline

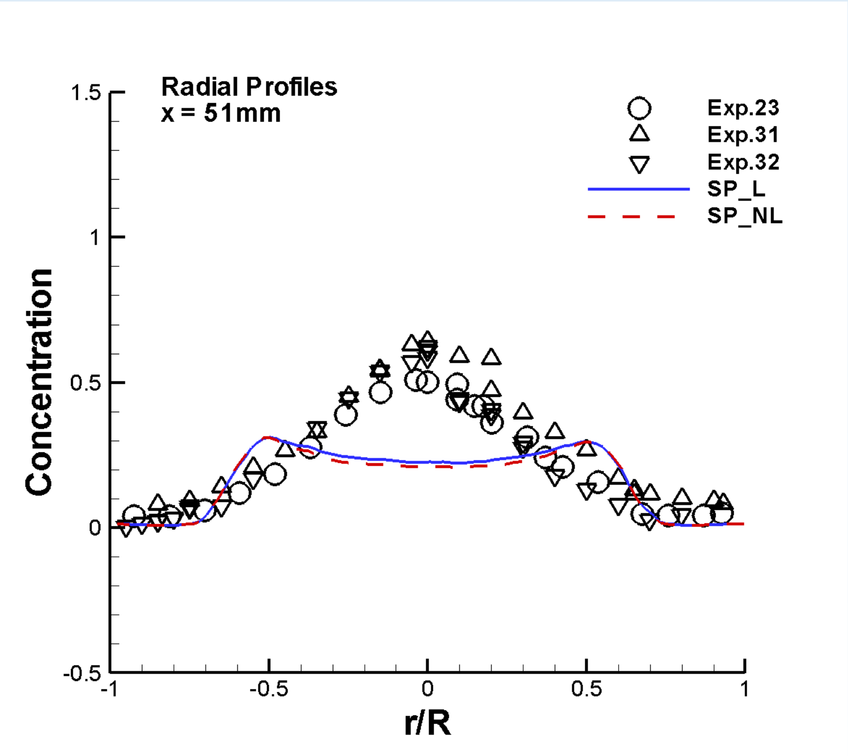

Inner Jet concentration at downstream

TFNS (VLES) simulation

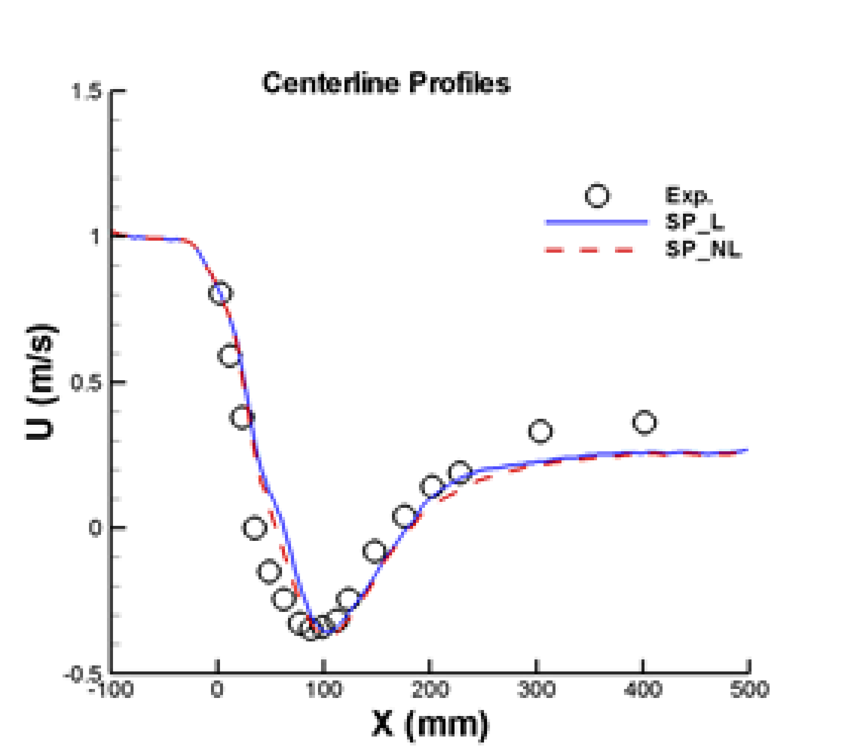

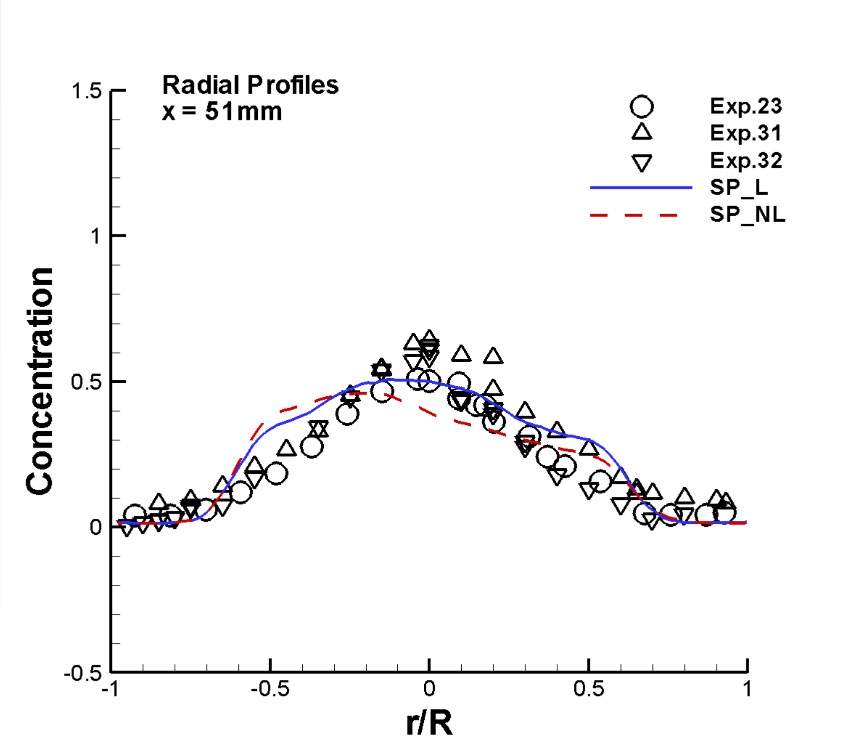

TFNS: Axial velocity along centerline

Inner Jet concentration at downstream

Hybrid TFNS/DWFDF vs. TFNS

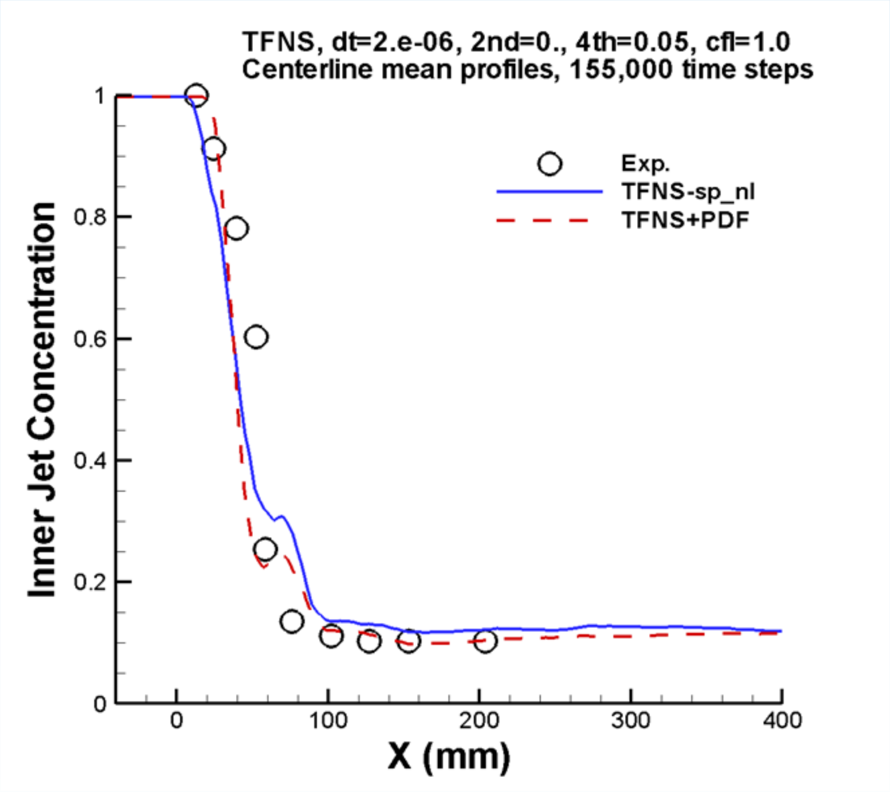

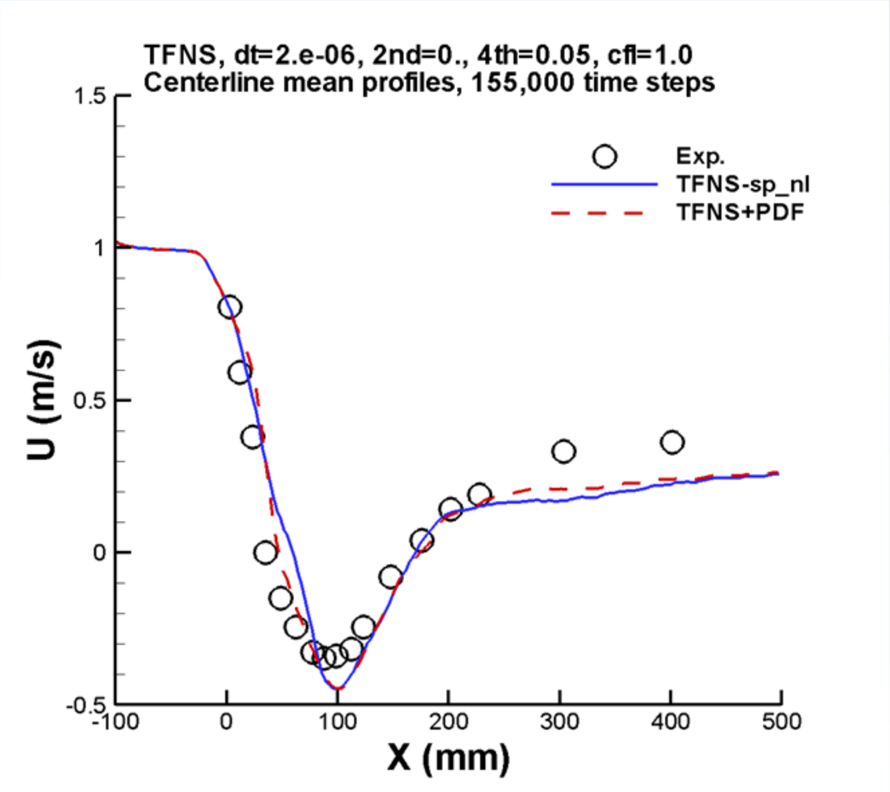

Mean concentration and axial velocity distribution along the centerline

Positive improvements shown from hybrid method

Appendix: RANS simulation
standard $k-\varepsilon$ model vs. nonlinear model

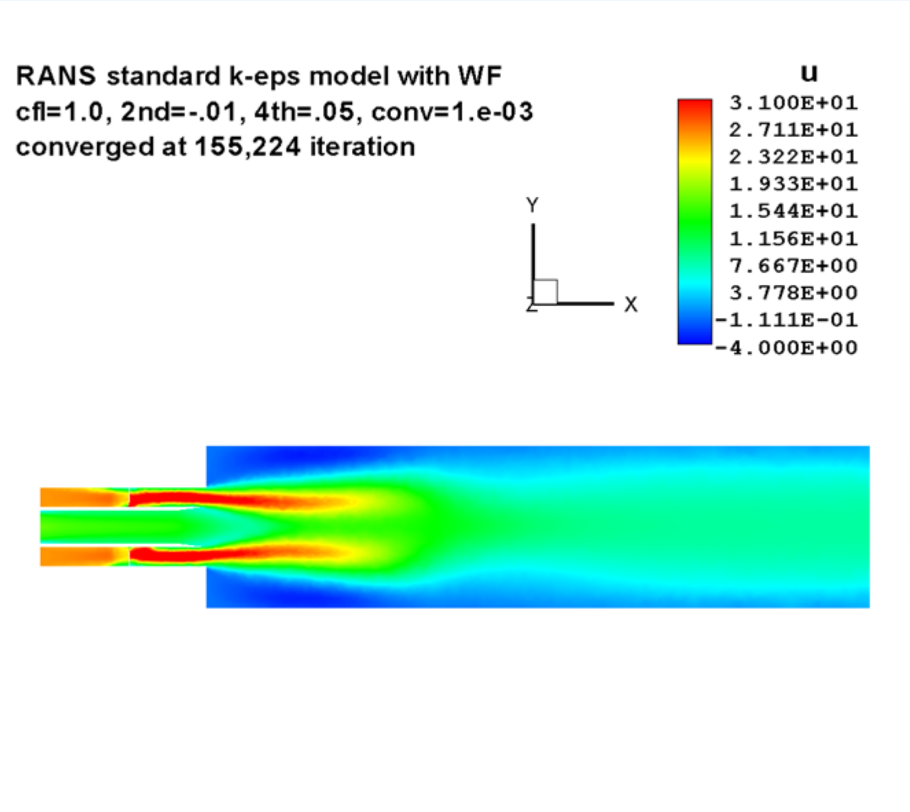

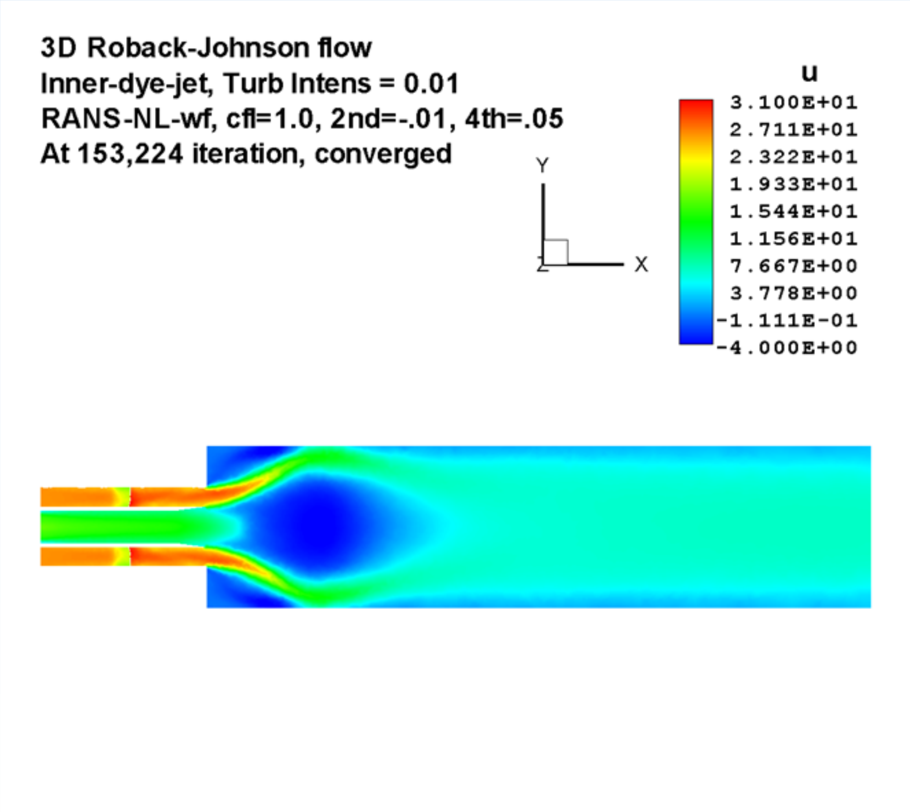

Center recirculation zone missed

Center recirculation zone

Appendix: RANS simulation standard $k-\varepsilon$ model vs. nonlinear model

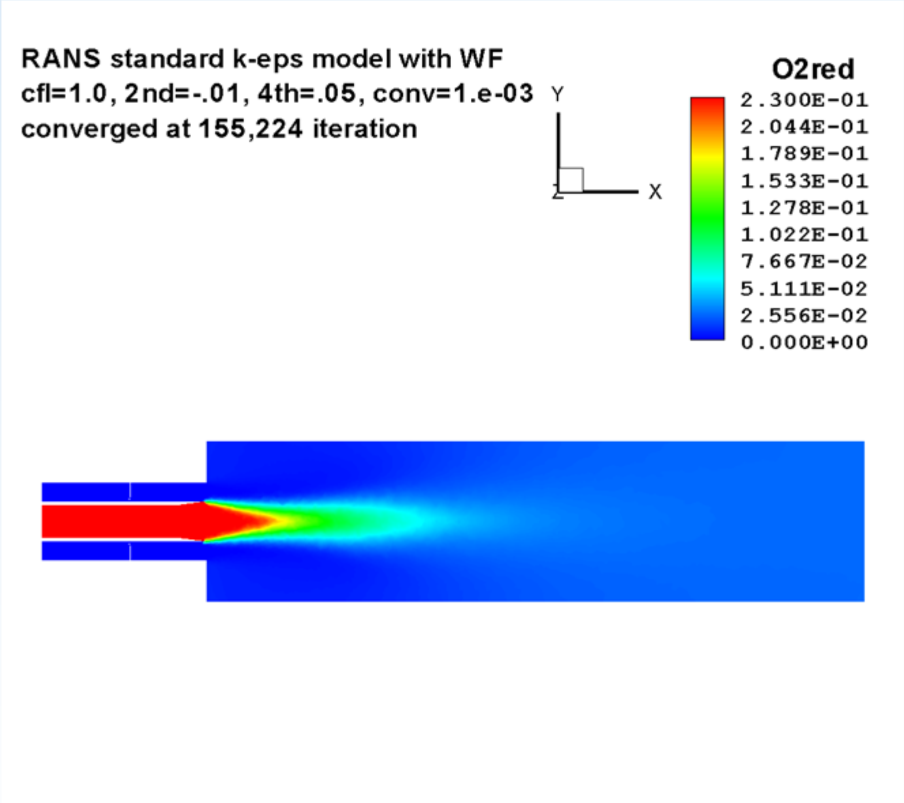

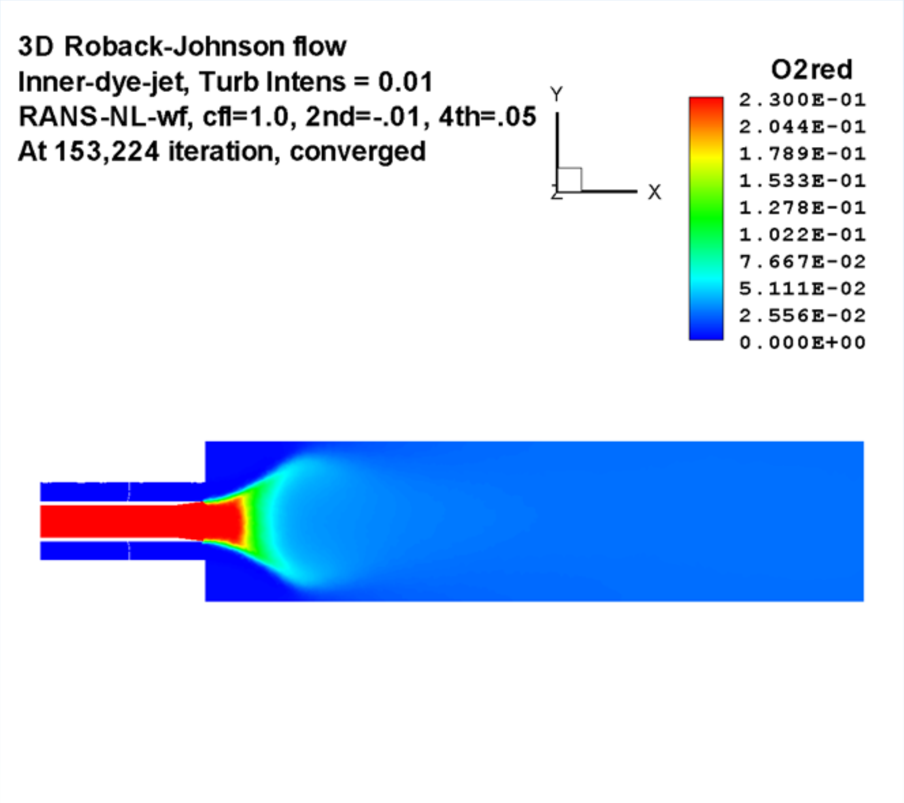

Contour of inner jet concentration at center plane (x,y)

Appendix: RANS simulation standard $k-\varepsilon$ model vs. nonlinear model

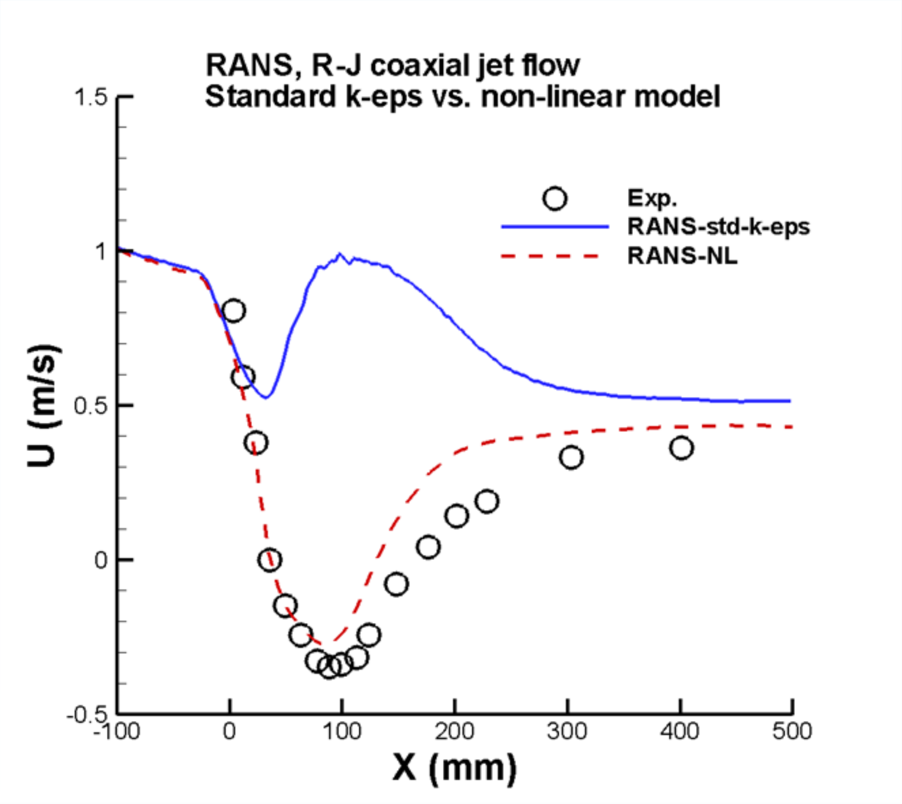

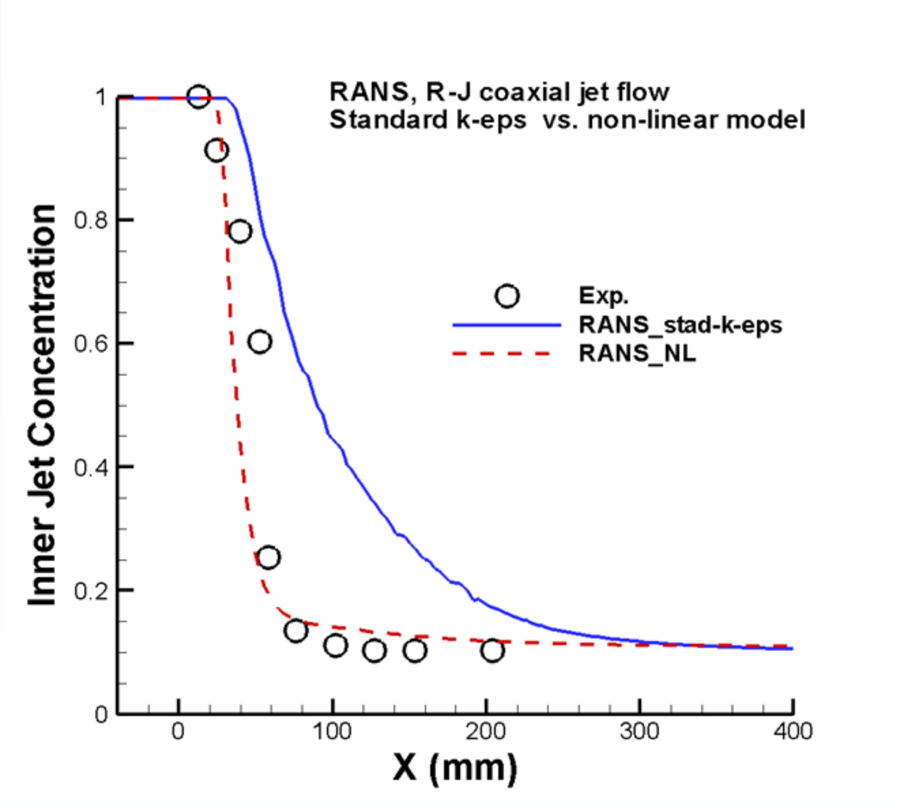

Axial velocity and concentration along the centerline

Conclusions

- Two groups of validations have been performed against experimental data:
  - The first group focuses on the turbulent scalar flux models: linear vs. nonlinear. Simulations include RANS, URANS and TFNS.
  - The second group focuses on the hybrid approach. Simulations include RANS/APDF, URANS/APDF and TFNS/DWFDF.
- Regarding the scalar flux model:
  - the linear and nonlinear scalar flux models have the same or similar behaves in RANS, URANS and TFNS simulations.
  - In the case of TFNS simulation, TFNS results demonstrate significant improvements over their RANS and URANS counter parts.
- Regarding the hybrid approach:
  - RANS/APDF, URANS/APDF and TFNS/DWFDF simulations show that they are quite close to their respective RANS, URANS and TFNS counterpart.
  - The hybrid approach appears to be more robust in the unsteady calculations and converge faster to use less computing time.
  - The above observations show a quite positive opinion of present hybrid PDF method for even non-reacting flow simulations.